

# Coronal element abundances of the post-common envelope binary V471 Tauri with *ASCA*

Martin Still<sup>1</sup>

*NASA/Goddard Space Flight Center, Code 662, Greenbelt, MD 20771*

Gaitee Hussain

*Harvard-Smithsonian Center for Astrophysics, 60 Garden Street, Cambridge, MA 02138*

## ABSTRACT

We report on *ASCA* observations of the coronally active companion star in the post-common envelope binary V471 Tau. Evolutionary calculations indicate that there should be no peculiar abundances on the companion star resulting from the common envelope epoch. Indeed, we find no evidence for peculiar abundances, although uncertainties are high. We find that a single-temperature plasma model does not fit the data. Two-temperature models with decoupled elemental abundances suggest that Fe is underabundant compared to the Hyades photospheric mean. In the absence of a measurement of photospheric Ne abundance in the cluster, we find Ne is overabundant compared to the solar photospheric value. This is indicative of the inverse first ionization potential effect. Differences between coronal and photospheric abundances are believed to result from the fractionation of ionized and neutral material in the upper atmosphere of the star.

*Subject headings:* binaries: close – stars: individual: V471 Tau – stars: magnetic fields – stars: white dwarfs – X-rays: binaries

## 1. Introduction

Solar observations have indicated that coronal abundances are photospheric for high-FIP (First Ionization Potential) elements, but that the coronal plasma is over abundant in low-FIP elements (Feldman 1992). Since low-FIP elements are ionized in the solar chromosphere, whereas high-FIP elements are not (Geiss 1992), it is believed that some mechanism separates ions from neutrals within the chromosphere and transports them to the corona. Hénoux 1995 provides a review of suggested mechanisms.

CCD X-ray detectors and proportional counting spectrographs have revealed multi-temperature stellar coronae with a variety of abundance distributions over ionization potential. Some show a FIP effect similar to the sun, others show the op-

posite trend - abundance decreasing with FIP relative to the solar photosphere, i.e. an inverse FIP effect. However, because of the moderate spectral resolutions available, combined with the confusion of line blending, much has been made of the possible ambiguity in abundance measurements using spectral models of collisionally-excited plasmas (Drake 1996).

The grating spectrographs onboard *EUVE* (Drake, Laming and Widing 1996), and recently launched on the *XMM-Newton* and *Chandra* satellites (Brinkman et al. 2001; Audard et al. 2001) have confirmed the general results of lower-resolution spectroscopy. Consequently, despite the poorer resolution compared to grating cameras and the possibility of line confusion, confidence in CCD and proportional counter measurements has increased. In this paper we present *ASCA* spectroscopy of the K star in the close binary

<sup>1</sup>Universities Space Research Association

V471 Tau, in order to measure its coronal content and contrast this with photospheric abundances.

V471 Tau is a member of the Hyades open cluster. Photospheric abundances of the Hyades members have been measured by Cayrel et al. (1985) and Varenne & Monier (1999) and some specific abundances of V471 Tau by Martín et al. (1997). Accepting model assumptions, we show in this paper that coronal Fe is under-abundant relative to the mean photospheric Hyades content and Ne is over-abundant, at least relative to the solar photosphere. This may be indicating that there is an inverse-FIP effect in the upper atmosphere of the star.

V471 Tau is a 12.5 hour eclipsing binary with a white dwarf and tidally-locked K2 companion (Nelson and Young 1970). At a distance of 47 pc (Werner & Rauch 1997), it is the closest object which has been through a recent common envelope phase of evolution. During the red giant phase of the white dwarf progenitor's life, the envelope of the giant was large enough to contain the orbit of the K star companion. While the two stars shared a common envelope, tides, friction and mass loss created a significantly smaller binary, with a short orbital period (Paczýnksi 1976). The envelope of the giant has since been ejected, but the binary still loses angular momentum through wind braking and gravitational radiation (Taam 1983). V471 Tau is therefore one of the best candidates for a pre-cataclysmic variable (pre-CV). CVs occur when the orbital period of a white dwarf-red dwarf binary becomes short enough for the main-sequence companion to fill it's Roche lobe. Quasi-persistent accretion will then occur through Roche lobe overflow. These objects are the sources of dwarf nova outbursts and classical nova eruptions that enrich the galactic ISM (Warner 1995).

Soft X-rays from V471 Tau were discovered by HEAO 1 (van Buren, Charles & Mason 1980) and it was detected as a flaring source by the *Einstein* Observatory (Young et al. 1983). This suggested that the K star was the source of X-rays, but by determining the white dwarf temperature to be 35,000 K using the *IUE* satellite, Guinan & Sion (1984) showed that the compact object may also be a significant X-ray emitter. Jensen et al. (1986) used *EXOSAT* to find white dwarf eclipses, pulsations, orbital dips and emission from both stellar components. Using the simultaneous

EUV/X-ray data from the *ROSAT* all-sky survey, Barstow et al. (1992) determined that the 555 s pulsations were the result of accretion caps on the white dwarf rather than g-mode oscillations. The interaction of rotating magnetic fields from the white dwarf and K star result in non-thermal emission at radio energies between the two objects (Patterson, Caillault & Skillman 1993; Lim, White & Cully 1996; Nicholls & Storey 1999). Possibly it is this magnetically ejected material that is accreted upon the white dwarf. Wheatley (1998) employed *ROSAT* to separate the K star from the white dwarf spectrally and pointed out that the K star flux was brighter than the average Hyades member but similar to the younger, faster rotators of the Pleiades. Therefore coronal luminosity in this source is probably related to rotation rate rather than age. The white dwarf is softer spectrally than the *ASCA* energy band, therefore it is not a factor during the analysis of the current data.

## 2. Observations

The Advanced Satellite for Cosmology and Astrophysics (*ASCA*; Tanaka, Inoue & Holt 1994) comprised four identical telescopes of nested thin foil reflectors (Serlemitsos et al. 1995). Four cameras were mounted at the focal planes. Two had Solid state Imaging Spectrometers (SIS0 and SIS1; Burke et al. 1991), and two carried Gas Imaging Spectrometers (GIS2 and GIS3) which were scintillation proportional counters (Ohashi et al. 1991). The SIS cameras have an energy range 0.4–10 keV, a spectral resolution of  $E/\Delta E = 20$  at 2 keV and a 22 arcmin field of view. The GIS instruments have an energy range 0.7–10 keV, a spectral resolution of  $E/\Delta E = 7.5$  at 2 keV and a 50 arcmin field of view.

Between MJD 50321.75 and MJD 50322.90 (1996 Aug 26-7), *ASCA* was pointed at V471 Tau for a total exposure time of 50 ksec, over 17 near-contiguous orbits. The *ASCA* sequence number of the observations is 24032000. The SIS cameras operated in FAINT mode and the data converted to BRIGHT mode, while GIS data was taken in PH mode with normal bit assignments.

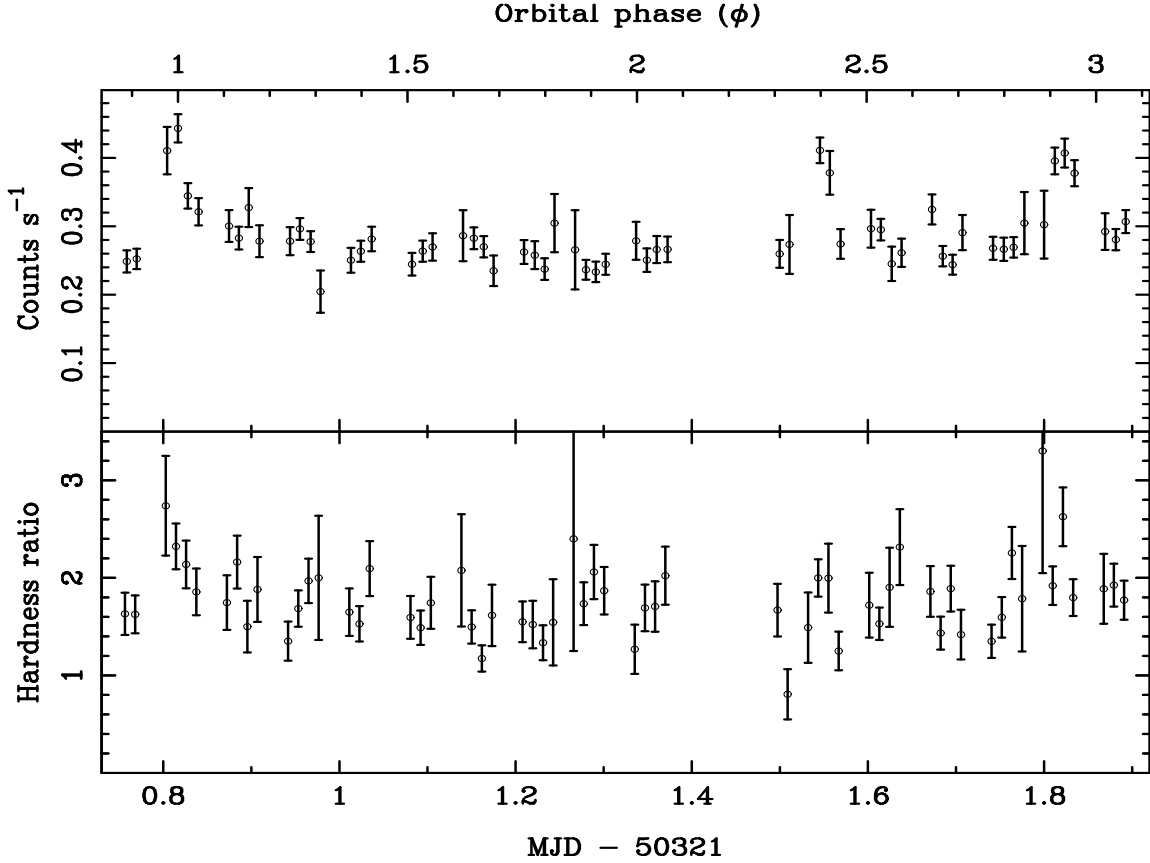


Fig. 1.— Top: the combined SIS and GIS 0.3–10 keV light curve for V471 Tau. Bottom: the hardness ratio between energy bands 0.3–1.0 keV and 1.0–10.0 keV. The orbital phase defined from the ephemeris of Guinan & Ribas (2001) is also provided. No emission is expected from the white dwarf at energies greater than 0.3 keV.

### 3. Analysis

Observations were screened using standard criteria and the FTOOLS software package v5.1. Events were filtered based on the satellite’s proximity to South Atlantic Anomaly passages, Earth elevation angle, pointing stability and rigidity of the geomagnetic field. Hot and flickering pixels were removed from the SIS events and we rejected particle events from the GIS observations. SIS data were additionally screened for proximity to the bright Earth-limb, time since the last passage over the day-night terminator, telemetry saturation and event rate. Only well-calibrated events, with grades 0, 2, 3 or 4 were retained. GIS data were additionally screened spatially to remove background ring and calibration source and further intervals of high particle background were clipped. A total of 41 ksec (SIS0), 44 ksec (SIS1), 48 ksec (GIS2) and 48 ksec (GIS3) of good data remained. The hot white dwarf component is softer spectrally than the *ASCA* energy band (Wheatley 1998), we find no evidence for it in the current data, and therefore we do not consider it in the

following analysis.

#### 3.1. Photometry

SIS event rates were determined within two spatially-distinct, circular region masks of diameter 8 arcmin and 5 arcmin for the source and background, respectively. Source events were extracted from the GIS tables within a circular region 12 arcmin in diameter and a background annulus 12–24 arcmin from the target. Background rates were normalized by the appropriate ratio of extraction areas and subtracted from the source events. The total SIS+GIS source event rate during the observation is provided in Fig. 1, averaged without weights into 1 ksec bins. We also provide the hardness ratio in the bands 0.3–1.0 keV and 1.0–10.0 keV.

Phases for each time bin were calculated using the orbital ephemeris of Guinan & Ribas (2001), converted to Modified Julian Date.

$$T = \text{MJD } 40\,609.564056(11) + 0.521183398(26) E \quad (1)$$

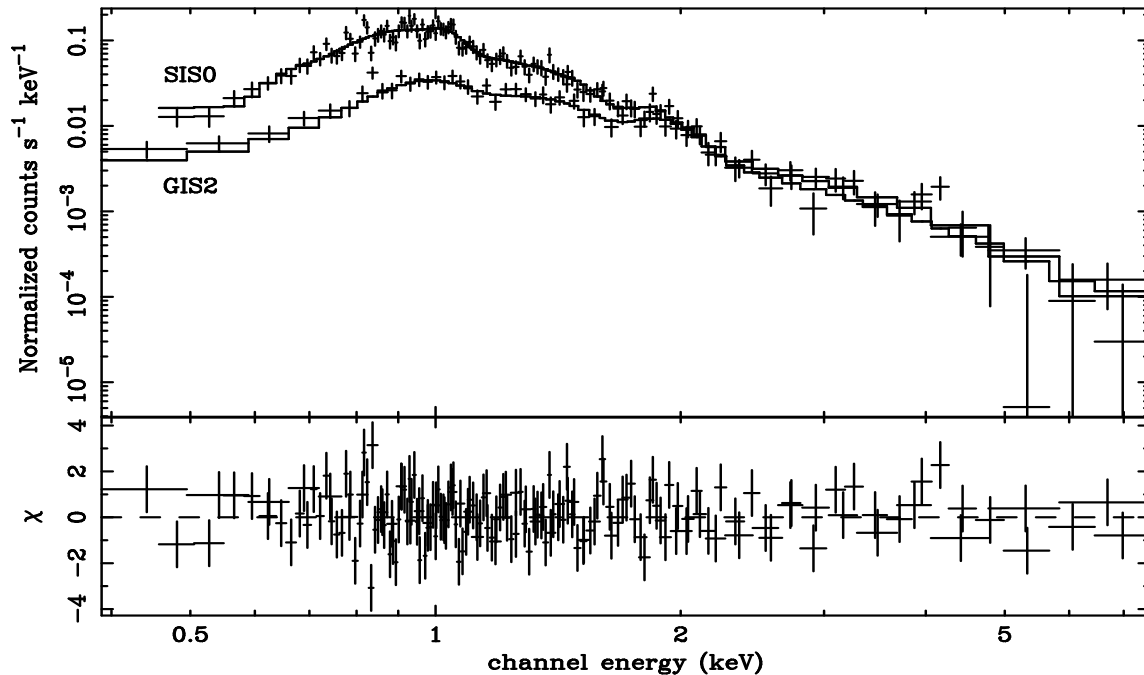


Fig. 2.— SIS0 and GIS2 spectra of V471 Tau with best fit. The model is an absorbed, optically thin, two temperature thermal plasma corresponding to Model 3 in Table 1.

where  $T$  is the average MJD of each bin and  $E$  is the cycle number. The orbital phase,  $\phi$ , in Fig. 1 corresponds to  $E - 18624$ . Quantities in parentheses correspond to  $1\sigma$  uncertainties.

Count rate is approximately constant, except for three flares, each of duration a few ksec at orbital phases  $\phi \simeq 1.0$ , 2.4 and 2.9. Statistically, the shape of the flares are not well-defined and there is only marginal evidence for spectral hardening. Flares of similar duration and amplitude are common to the rapidly rotating stars in tidally-locked binaries, e.g., the RS CVn systems (Francosini, Pallavicini & Tagliaferri 2003), and to single M dwarf stars (Tsikoudi & Kellett 2000). The observed flares do not occur at preferred orbital phases.

V471 Tau is relatively faint compared to most well-observed coronal sources (e.g. Brinkman et al. 2001, Audard et al. 2001), so in order to maximize counting statistics during spectral fitting, we do not separate flare events from the quiescent data.

### 3.2. Spectroscopy

To improve the accuracy of  $\chi^2$  fitting, the SIS and GIS energy channels containing less than 30 events were grouped with their neighbors. Channels flagged as bad were rejected and those with corrected pulse heights of  $0.3 > E > 10$  keV were ignored. Best fits to the data were determined using the APEC thermal plasma model (Brickhouse et al. 2000), absorbed through a neutral interstellar column with photo-electric cross-sections provided by Balucinska-Church & McCammon (1992). Spectra from all four cameras were employed together to converge on a single model.

The APEC code (v1.10) contained within the current version of the spectral fitting package, XSPEC v11.2, does not include high  $n$  transitions of Fe XVII–XIX. Also there are systematic problems in line wavelengths for the set of Ni lines in this version. Therefore additional tables for Fe XVII;  $n = 6, 7$  and  $8 \rightarrow 2$ , Fe XVIII;  $n = 6, 7 \rightarrow 2$  and Fe XIX;  $n = 6 \rightarrow 2$  are included together with a table of corrected Ni wavelengths, as described in Brickhouse et al. (2000). Since these models are additive, abundances cannot be decoupled from model

TABLE 1

SPECTRAL FIT PARAMETERS FOR FOUR THERMAL PLASMA MODELS. ABUNDANCES ARE PROVIDED AS THE LOGARITHMIC VALUE OF THE RATIO BETWEEN CORONAL AND SOLAR PHOTOSPHERIC VALUES, RELATIVE TO H. THE ABUNDANCES OF SOME OF THE ELEMENTS, C, N, AL, S, AR, CA AND NI, WERE NOT WELL CONSTRAINED BY THE DATA. MODELS ARE IDENTICAL EXCEPT FOR DIFFERENT ASSUMED ABUNDANCES FOR THE ELEMENTS ABOVE. BEST FIT ABUNDANCES IN THE *ASCA* BAND ARE PROVIDED FIRST, WITH THE TEMPERATURES AND EMISSION MEASURES, ASSUMING A TWO-TEMPERATURE EMISSION REGION, SECOND. UNCERTAINTIES ARE 90 PERCENT CONFIDENCE LIMITS FOR EACH QUANTITY, ALL FIT PARAMETERS WERE FREE TO VARY DURING THE UNCERTAINTY CALCULATIONS. THE  $\chi^2$  OF EACH FIT AND NUMBER OF DEGREES OF FREEDOM ARE PROVIDED AT THE BOTTOM.

Element	FIP (eV)	Model 1 <sup>a</sup>	Model 2 <sup>b</sup>	Model 3 <sup>c</sup>	Model 4 <sup>d</sup>
[Mg/H]	7.65	$-0.23^{+0.12}_{-0.06}$	$0.07^{+0.38}_{-0.25}$	$-0.06^{+0.29}_{-0.21}$	$0.38^{+0.25}_{-0.18}$
[Fe/H]	7.87	$-0.23^{+0.12}_{-0.06}$	$-0.17^{+0.29}_{-0.12}$	$-0.19^{+0.17}_{-0.13}$	$-0.17^{+0.33}_{-0.25}$
[Si/H]	8.15	$-0.23^{+0.12}_{-0.06}$	$0.02^{+0.33}_{-0.19}$	$-0.12^{+0.24}_{-0.23}$	$0.32^{+0.20}_{-0.17}$
[O/H]	13.61	$-0.23^{+0.12}_{-0.06}$	$-0.07^{+0.47}_{-0.35}$	$-0.05^{+0.28}_{-0.35}$	$0.27^{+0.36}_{-0.25}$
[Ne/H]	21.56	$-0.23^{+0.12}_{-0.06}$	$0.51^{+0.35}_{-0.20}$	$0.38^{+0.26}_{-0.25}$	$0.78^{+0.22}_{-0.19}$

Parameter	Model 1 <sup>a</sup>	Model 2 <sup>b</sup>	Model 3 <sup>c</sup>	Model 4 <sup>d</sup>
$kT_1$ <sup>e,f</sup>	$0.78^{+0.03}_{-0.02}$	$0.67^{+0.07}_{-0.07}$	$0.71^{+0.06}_{-0.12}$	$0.67^{+0.08}_{-0.07}$
$EM_1$ <sup>g</sup>	$3.05^{+0.82}_{-0.88}$	$2.02^{+1.13}_{-1.02}$	$2.30^{+1.24}_{-0.91}$	$1.08^{+0.47}_{-0.46}$
$kT_2$ <sup>e,f</sup>	$1.93^{+0.18}_{-0.16}$	$2.51^{+0.49}_{-0.37}$	$2.45^{+0.37}_{-0.38}$	$2.57^{+0.48}_{-0.24}$
$EM_2$ <sup>g</sup>	$3.00^{+0.32}_{-0.37}$	$1.99^{+0.51}_{-0.77}$	$2.60^{+0.85}_{-0.04}$	$1.26^{+0.20}_{-0.24}$
$\chi^2$ (dof)	414(341)	380(336)	377(335)	383(336)

<sup>a</sup>Metal abundances all equal.

<sup>b</sup>Metal abundances equal to Fe, except Mg, Si, O and Ne.

<sup>c</sup>Metal abundances equal, except Mg, Fe, Si, O and Ne.

<sup>d</sup>Metal abundances equal to the Hyades photospheric mean, except Mg, Fe, Si, O and Ne.

<sup>e</sup>Temperature (keV).

<sup>f</sup>Neutral hydrogen column density was taken to be  $\log N_{\text{H}} = 18.7$  (Jensen et al. 1986).

<sup>g</sup>Emission measure ( $10^{52} \int n_e n_{\text{H}} dV$ )  $\text{cm}^{-3}$ ;  $n_e$  is the electron density,  $n_{\text{H}}$  the hydrogen plasma density and  $dV$  the emitting volume. Source distance is taken to be 47 pc (Werner & Rauch 1997).

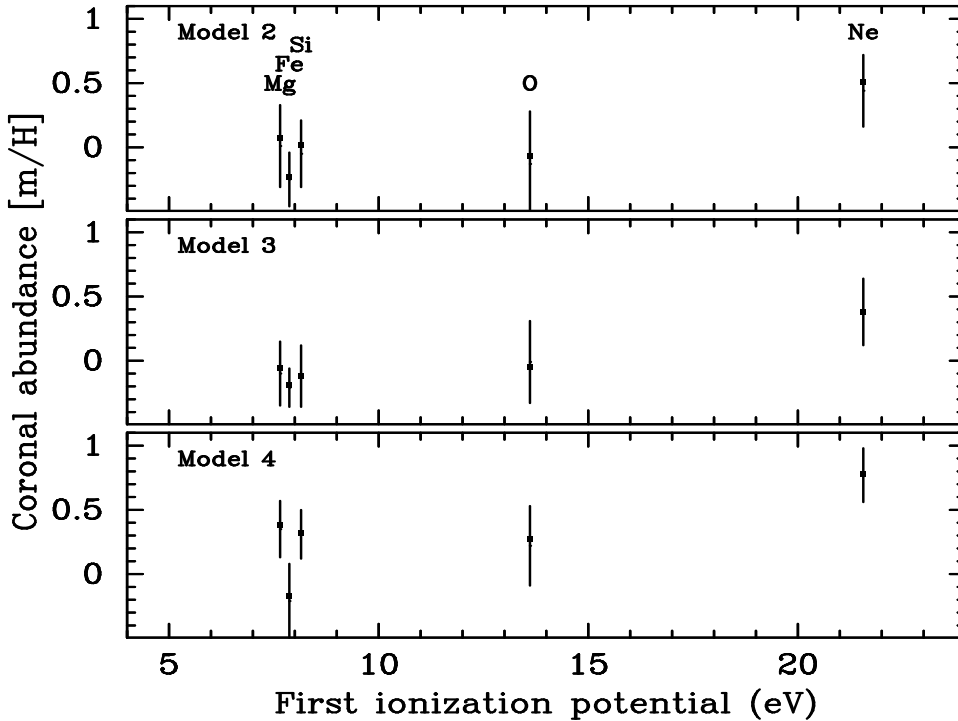


Fig. 3.— Coronal elemental abundances from Models 2, 3 and 4, showing a relative overabundance of Ne in each case. Error bars are 90 percent confidence ranges.

normalizations in these two cases. Although these models avoid errors in fitting high- $n$  Fe and Ni, they cannot be used to measure abundances.

If all abundances are allowed to roam as independent fit parameters, then a statistically significant constraint on any individual element is not possible using this data set. By trial and error we find that significant detections of Mg, Fe, Si, O and Ne (with H-like transitions at the peak of the *ASCA* response) are made if we adopt some reasonable assumptions concerning the fractions of the other elements contributing to the line spectrum, i.e., C, N, Al, S, Ar and Ca. Consequently we describe below four abundance models. Solar abundance values were taken from Grevesse & Sauval (1998).

Model 1 assumes the abundances of all metals are equal; in this case the abundance is dominated by the L shell lines of Fe. Model 2 allows the abundances of Mg, Si, O and Ne to float as free parameters while the others are floating but assumed equal. The combined metal abundance will again be dominated by Fe. Model 3 is similar to model 2 except that the Fe abundance is de-

coupled from the combined elements and allowed to float on its own. The remaining abundances of C, N, Al, S, Ar and Ca float, but are equal. Model 4 is identical to model 3 except C, N, Al, S, Ar and Ca are fixed abundances with the mean photospheric value of the Hyades members ( $[m/H] = +0.1$ ; Martín, Pavlenko and Rebolo 1997, where  $[m/H]$  is the logarithmic ratio of the element abundance,  $m$ , and H abundance, relative to solar).

Realistically, we expect a whole range of plasma temperatures and, unsurprisingly, single-temperature models provide poor fits to the data with  $\chi^2 = 571$  for 337 d.o.f. (model 3). Two-temperature models yield statistically significant fits although they are still undoubtedly a simplification of the temperature structure. Table 1 lists the best fit parameters and  $\chi^2$  statistic for each model. All models are acceptable according to the  $\chi^2$  statistic so we cannot adopt a best-model and can generalize the results only.

Between Models 2, 3 and 4 we find general consistency between temperatures and emission measures. If the neutral hydrogen column density was left as a free parameter, in all cases it was found

to be both consistent with zero and smaller than the total galactic column in that direction ( $1.58 \times 10^{21} \text{ cm}^{-2}$ ; Dickey & Lockman 1990). However, since the *ASCA* energy range is not well suited for the measurement of the expected column in front of V471 Tau, we adopt the value derived from *EXOSAT* measurements by Jensen et al. (1986) of  $N_{\text{H}} = 5 \times 10^{18} \text{ cm}^{-2}$ . The flux from the source according to these models is  $2.4 \times 10^{-12} \text{ ergs}^{-1} \text{ cm}^{-2}$ .

For each model, Fe abundance is most-likely sub-solar, the opposite to the solar corona, whereas Ne is greater than solar. In Fig. 2 we show the best-fit model 3, folded on the energy-resolved count rates from SIS0 and GIS2 and their residuals. Although far from conclusive, the high Ne/Fe ratio is suggestive of an inverse-FIP effect. For models 2, 3 and 4, the coronal abundances of the five significantly-constrained elements are plotted against FIP in Fig. 3.

#### 4. Discussion

For various model assumptions, we have determined the element abundances of Mg, Fe, Si, O and Ne in the corona of V471 Tau and demonstrated a high Ne/Fe ratio which could be indicative of the inverse-FIP effect. In the following section, we ask whether we expect to find fossil abundances from the post common envelope epoch. We also discuss the proposed mechanisms behind the FIP effect and, finally, compare the coronal abundances with the measured photospheric abundances of dwarf stars in the Hyades cluster.

##### 4.1. Common envelope abundances

During the white dwarf progenitor’s red giant phase of evolution, the two stars shared a common envelope and, therefore, there was element mixing between them. Using LTE atmosphere fits to optical spectroscopy of V471 Tau, and providing NLTE corrections, Martín et al. (1997) found photospheric abundances consistent with the Hyades,  $[m/\text{H}] = +0.1$ , in Al, Ca, Fe and Si. The one exception was Li, where  $[\text{Li}/\text{H}] = 2.4 \pm 0.3$ . This is greater than a factor  $10^2$  more abundant than normal Hyades members. Although Li is usually depleted in convection layers, Martín et al. argue that the rapid rotation of the K star maintains the

fossil level of Li after sharing a common envelope phase with the Li-rich giant (de la Reza, Drake & da Silva 1996). Unfortunately there are no Li transitions in the *ASCA* energy band to test this independently.

Marks & Sarna (1998) calculate the evolution of photospheric abundances on the companion star of cataclysmic variables, including the effects of a common envelope epoch. They indicate that, indeed, photospheric abundances in the K star are expected to remain unchanged through the common envelope phase, and remain constant thereafter until the white dwarf accretion rate is sufficient to drive a cycle of nova eruptions. Therefore we do not expect to find evidence for the common envelope phase in the current measurements, however, peculiar abundances may yet be present if the proposed *IUE* detection of expanding nova material around V471 Tau by Bruhweiler & Sion (1986) and Sion et al. (1989) is confirmed. However subsequent *HST* spectroscopy shows no indication of shell features but does detect transient coronal ejection events (Bond et al. 2001). These may well have been mistaken for an expanding shell before coronal ejections were time-resolved by *HST*. In light of both the observational and theoretical evidence, we will assume that the photospheric abundances of the companion star in V471 Tau are identical to the average Hyades dwarf. This is useful later for comparing the coronal and photospheric abundances.

##### 4.2. FIP bias

Observations have indicated that the coronal, energetic particle and cosmic ray abundances in the sun are all different from the solar photospheric content (Meyer 1985a,b). This is probably equally true for active stars (Brinkman et al. 2001; Audard et al. 2003). While in most cases the photospheric abundances remain uncertain, there is at least one strong piece of evidence for fractionation regions in between stellar photospheres and coronae. It derives from the fact that coronal abundances are correlated with elemental FIP. In the solar atmosphere the ratio of coronal to photospheric abundances decreases with FIP. When comparing stellar coronal abundances to the solar photosphere some sources follow this trend while others show the “inverse FIP effect”, i.e. an increasing ratio with increasing FIP (Brinkman

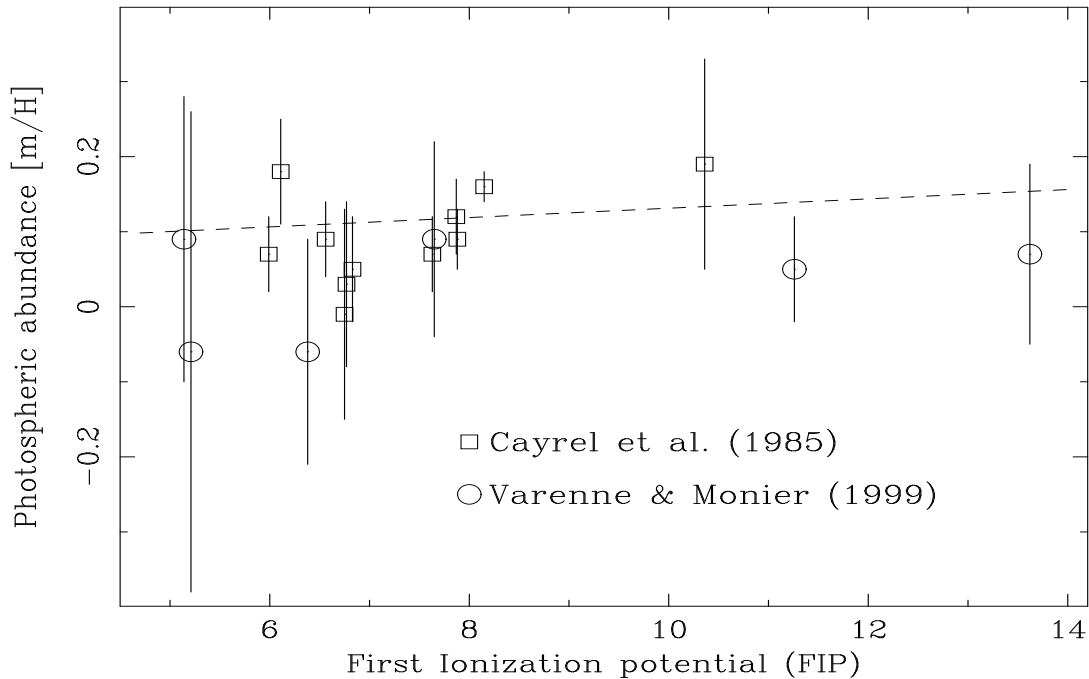


Fig. 4.— Mean photospheric abundances of Hyades dwarfs (Cayrel et al. 1985; Varenne & Monier 1999) plotted as function of FIP. The line is the best linear fit to the data.

et al. 2001). The Ne/Fe ratio in V471 Tau is suggestive of an inverse-FIP trend.

FIP effects are thought to be directly associated with the process of element fractionation in stellar atmospheres (Hénoux 1995). The ionized fraction of each element will depend on the plasma temperature in the fractionation region. Some process is required to decouple the ionized and neutral plasmas. Possibly the charged particles are accelerated along field lines in loops above the stellar photosphere (Wang 1996). Flare ejection provide another mechanism to propel material into the corona (Schmelz 1993). The abundances of coronal elements as a function of FIP has been observed to change during X-ray flares. Audard, Güdel & Mewe (2001) find an inverse FIP affect in HR 1099 during quiescence but a quenching of this effect during flares.

#### 4.3. Abundances in the Hyades

Abundances in most stellar photospheres are not well known. Instead, it is common practice to compare stellar coronal abundances with the solar photosphere. Rather than adopting solar photospheric abundances, ideally we would prefer to

have direct measurements of photospheric abundances in the K companion of V471 Tau in order to make an unbiased comparison between photosphere and corona. These are poorly determined generally because of uncertainties in galactic element mixing and the details of stellar spectral synthesis models. Fortunately, though, V471 Tau is a member of the nearest open cluster, the Hyades (Werner & Rauch 1997), where photospheric abundances are considerably better determined than most coronal X-ray sources.

Metallicities in open clusters are indicators of the quantity and rate of chemical mixing in the galaxy. However stellar abundance determinations are generally plagued by a wide range of biases (see e.g. Griffin & Holweger 1989). Various techniques have consequently supplied abundances for the Hyades cluster ranging from  $[\text{Fe}/\text{H}] = -0.09$  (Tomkin & Lambert 1978) to  $[\text{Fe}/\text{H}] = +0.42$  (Gustafsson & Nissen 1972).

Although not unequivocally free of bias, Cayrel, Cayrel de Strobel & Campbell (1985) determine a mean  $[\text{Fe}/\text{H}]$  enhancement over solar of  $+0.12 \pm 0.03$  using high dispersion spectroscopy of a sample of 12 Hyades dwarfs distributed tightly about



the solar spectral type. This result was determined by comparison of the curve of growth over the linear and saturated branches of FeI lines with photospheric spectral models. A large surface fraction of active regions over these stars would probably result in an under-estimate of the abundance, but an identical estimate of  $[\text{Fe}/\text{H}] = +0.14 \pm 0.01$  from a smaller sample of FeII lines suggests that any bias due to chromospheric activity is small among the measured cases. While systematic errors may still be present, this result has been confirmed with a sample of F stars with  $v \sin i < 30 \text{ km s}^{-1}$  by Boesgaard (1989), finding  $[\text{Fe}/\text{H}] = +0.13 \pm 0.03$ . Consequently, by comparison with the *ASCA* results, Fe abundance is higher in the photosphere compared to the corona of V471 Tau, within the uncertainties.

Cayrel et al. (1985) provide coronal abundances for Si;  $[\text{Si}/\text{H}] = +0.16 \pm 0.04$ . Varenne & Monier (1999) present photospheric O abundances for 26 F stars in the Hyades with an average value of  $[\text{O}/\text{H}] = +0.07$ . In these cases there are no significant differences between the coronal and photospheric populations, but the coronal abundances are poorly defined using the current data. However, as in other sources (e.g. Brinkman et al. 2001), the suggestion of a coronal FIP bias in V471 Tau hinges crucially on the measurement of Ne.

Critically, photospheric Ne has not been measured in the Hyades because the low photospheric temperatures do not provide an environment for noble gas emission. We combine the Hyades abundances from Cayrel et al. and Varenne & Monier in Fig. 4. We do not include the two stars in the Cayrel et al. sample that are thought to be active sources. Data points from a sample of cluster members have been averaged and uncertainties obtained by calculating the standard deviations for each species. A linear least-squares fit yields  $[\text{m}/\text{H}] = 0.069_{-0.140}^{+0.140} + 0.006_{-0.017}^{+0.018} E$ , where  $E$  is the FIP in eV. Uncertainties are the 90 percent confidence limits, i.e. the abundances are consistent with a flat distribution across the range of FIP.

We fit the slope of the X-ray FIP distributions from Fig. 3, including the Ne data. Clearly the FIP-trend is consistent with a constant if Ne is ignored. Least-square fitting yields slopes consistently of  $0.04 \pm 0.03$  for models 2, 3 and 4. Un-

certainties are 90 percent confidence limits. Consequently, with Ne included, the coronal FIP distribution is steeper than the Hyades mean photospheric distribution.

## 5. Conclusion

We have measured model-dependent coronal abundances of Mg, Fe, Si, O and Ne in the corona of the post-common envelope binary V471 Tau. A single-temperature plasma model does not fit the data adequately. Binary evolution calculations have predicted that we would see no symptoms of element mixing during the common-envelope epoch and we indeed find no evidence for it; i.e., abundances are not unusual compared to the coronae of single stars or wide binaries. In all likelihood, the coronal Fe abundance is significantly less than the Hyades photospheric mean. This is in direct contrast to the ratio of Fe in the solar corona which is overabundant relative to the solar photosphere. There is evidence for an inverse FIP bias, although this relies entirely on our measurement of coronal Ne abundance. Due to the lack of low-ionization Ne lines in the optical band, the photospheric abundance of this element cannot be directly compared to the coronal value, adding further uncertainty. While CCD spectroscopy is not currently an ideal method for abundance determination, these data indicate that V471 Tau is a viable and interesting target for the grating instruments on-board the *Chandra* and *XMM-Newton* observatories for such a purpose.

This paper was based on data obtained from the High Energy Astrophysics Science Archive Research Center (HEASARC), provided by NASA's Goddard Space Flight Center. We thank Nancy Brickhouse for supplying additional Fe and Ni atomic data.

## REFERENCES

- Audard M., Güdel M., Mewe R., 2001, *A&A*, 365 L318
- Audard M., Güdel M., Sres A., Raassen A.J.J., Mewe R., 2003, *A&A*, 398, 1137
- Balucinska-Church M., McCammon D., 1992, *ApJ*, 400, 699

- Barstow M.A., Schmidt J.H.M.M., Clemens J.C., Pye J.P., Denby M., Harris A.W., Pankiewicz G.S., 1992, MNRAS, 255, 369
- Boesgaard A.M., 1989, ApJ, 336, 798
- Bond H.E., Mullan D.J., O'Brien M.S., Sion E.M., 2001, ApJ, 560, 919
- Brickhouse N.S., Dupree A.K., Edgar R.J., Liedahl D.A., Drake S.A., White N.E., Singh K.P., 2000, ApJ, 530, 387
- Brinkman A.C. et al., 2001, A&A, 365, L324
- Bruhweiler F.C., Sion E.M., 1986, ApJ, 304, L21
- Burke B.E. et al., 1991, IEEE Trans., ED-38, 1069
- Cayrel R., Cayrel de Strobel G., Campbell B., 1985, A&A, 146, 249
- de la Reza R., Drake N.A., da Silva L., 1996, ApJ, 456, L115
- Dickey J.M., Lockman F.J., 1990, ARA&A, 28, 215
- Drake J.J., Laming J.M., Widing K.G., 1996, p. 97 in Bowyer S. Malina R.F. eds., Astrophysics in the extreme ultraviolet, IAU Colloquium 152, Kluwer: Dordrecht
- Drake S.A., 1996, p. 215 in Holt S.S., Sonneborn G., eds., Proceedings of the sixth (6th) annual October Astrophysics Conference in College Park, Maryland, ASP Conference Series Vol. 99
- Feldman U., 1992, Phys. Scripta, 46, 202
- Franciosini E., Pallavicini R., Tagliaferri G., 2003, A&A, 399, 279
- Geiss J., 1982, Space Sci. Rev., 33, 201
- Grevesse N., Sauval A.J., 1998, Space Sci. Rev. 85, 161
- Griffin R.E.M., Holweger H., 1989, A&A, 214, 249
- Guinan E.F., Ribas I., 2001, ApJ, 546, 43L
- Guinan E.F., Sion E.M., 1984, AJ, 89, 1252
- Gustafsson B, Nissen P.E., A&A, 19, 261
- Hénoux J.-C., 1995, Adv. Space Res., 15, (7)23
- Jensen K.A., Swank J.H., Petre R., Guinan E.F., Sion E.M., Shipman H.L., 1986, ApJ, 309, L27
- Lim J. White S.M., Cully S.L., 1996, ApJ, 461, 1009
- Marks P.B., Sarna M.J., 1998, MNRAS, 699, 720
- Martín E.L., Pavlenko Y., Rebelo R., 1997, A&A, 326, 731
- Meyer J.-P., 1985a, ApJS, 57, 173
- Meyer J.-P., 1985b, ApJS, 57, 151
- Nelson B., Young A., 1970, PASP, 82, 699
- Nicholls J., Storey M.C., 1999, ApJ, 519, 850
- Ohashi T. et al., 1991, Proc. SPIE, 1549, 9
- Paczýnski B., 1976, p. 75 in Eggleton P., Mitton S., Whelan J., eds., Structure and Evolution of Close Binary Systems, IAU Symposium no. 73, Reidel: Dordrecht
- Patterson J., Caillault J.-P., Skillman D.R., 1993, PASP, 105, 848
- Schmelz J.T., 1993, ApJ, 408, 373
- Serlemitsos P. et al., 1995, PASJ, 47, 105
- Sion E.M., Bruhweiler F.C., Mullan D., Carpenter K., 1989, ApJ, 341, L17
- Taam R.E., 1983 ApJ, 268, 361
- Tanaka Y., Inoue H., Holt S.S., 1994, PASJ, 46, L37
- Tomkin J., Lambert D.L., 1978, ApJ, 223, 937
- Tsikoudi V., Kellett B.J., 2000, MNRAS, 319, 1147
- van Buren D., Charles P.A., Mason K.O., 1980, ApJ, 242, L105
- Varenne O., Monier R., 1999, A&A, 351, 247
- Wang Y.-M., 1996, ApJ, 464, L91
- Warner B., 1995, Cataclysmic Variable Stars, CUP: Cambridge
- Werner K., Rauch T., 1997, A&A, 324, L25
- Wheatley P.W., 1998, MNRAS, 297, 1145

Young A., Klimke A., Africano J.L., Quigley R.,  
Radick R.R., van Buren D., 1983, ApJ, 267, 655

---

This 2-column preprint was prepared with the AAS L<sup>A</sup>T<sub>E</sub>X  
macros v5.0.